TEPES
TURKISH JOURNAL OF
ELECTRICAL POWER
AND ENERGY SYSTEMS

TEPES, Vol. 3, Issue. 1, 39-46, 2023 **DOI:** 10.5152/tepes.2023.23002

RESEARCH ARTICLE

Economic and Environmental Analysis of Grid-Connected Rooftop Photovoltaic System Using HOMER

Mikail Pürlü, Umut Özkan

Department of Electrical and Electronic Engineering, Sivas Cumhuriyet University, Sivas, Turkey

Cite this article as: M. Pürlü, U. Özkan, "Economic and environmental analysis of grid-connected rooftop photovoltaic system using HOMER," *Turk J Electr Power Energy Syst.*, 2023; 3(1), 39-46.

ABSTRACT

Due to the increasing energy demand and the climate crisis in the world, the importance of alternative energy generation techniques, which are clean and cheap, is increasing. Since renewable energy sources are clean and sustainable, their integration into the grids at transmission or distribution levels as distributed generation sources provides significant benefits both economically and environmentally. Rooftop solar panels are also an application of small-power renewable distributed generation technologies. In this study, the economic and environmental analysis of the rooftop photovoltaic system designed to increase the green energy usage rate and reduce the greenhouse gases released to the environment has been made. Considering the electricity consumption data and roof area of an office building of a factory located in the north of Turkey, solar radiation data obtained from three different sources such as the General Directorate of Meteorology, National Aeronautics and Space Administration, and Photovoltaic Geographical Information System were used during the analyses carried out in the Hybrid Optimization Models for Energy Resources program. By providing an annual average of 160 000 kWh (11%) clean energy generation, the annual release of pollutants such as 101.353 kg of carbon dioxide, 0.439 kg of sulfur dioxide, and 0.215 kg of nitrogen oxide to the environment has been prevented.

Index Terms— HOMER, grid connected, renewable energy.

I. INTRODUCTION

The world has been struggling with two major problems, energy crisis and climate crisis, for decades [1]. Microgrid and nanogrid applications, in which renewable energy sources (RESs) are integrated, have become increasingly popular in order to meet the increasing energy demand of societies with large populations and reduce their carbon footprint. Off-grid (standalone) hybrid energy systems (HES), which are independent of the grid and include RESs, non-renewable energy sources, and energy storage systems (ESSs) together, are one of the most suitable solutions for electrification of undeveloped or rural areas that are far from the grid or where there is no electricity grid. On-grid (grid-connected) HESs are designed with concerns such as increasing the renewable fraction, emission mitigation, voltage profile improvement, technical loss reduction, and meeting energy demand reliably.

HESs include RESs such as solar, wind, biomass, and geothermal and hydro energy, fossil fuel-based production technologies such as diesel generator (DG), and ESSs such as batteries, pumped storage, and flywheel, which are suitable for the design region. The selection, sizing, and placement of the correct components are performed as a result of the analyses made to provide technical, economic, and environmental contribution.

Many optimization algorithms and tools are used to design HESs. Also, various computer simulation software are available to analyze HESs, and their features can be summarized as in Table I [2].

In order to provide cheaper electricity to Burkina Faso, off-grid microgrid design including battery, photovoltaic (PV), maximum power point tracking, and inverter has also been realized in Hybrid Optimization Models for Energy Resources (HOMER) pro [3]. A renewable HES based on PV/fuel cell/battery energy storage system (BESS) to support the irrigation of paddy fields in Bihar, India, was designed and modeled in the LabVIEW environment [4]. Using genetic algorithm, particle swarm optimization algorithm, and artificial bee colony algorithms, the authors in [5] designed a HES with PV/BESS/DG for a region in Southwest Nigeria. In [6], off-grid and

Corresponding author: Mikail Pürlü, **E-mail:** mikailpurlu@cumhuriyet.edu.tr

Received: January 2, 2023
Accepted: January 11, 2023
Available online: February 15, 2023

TABLE I.
SIMULATION PROGRAMS FOR THE DESIGN OF ENERGY SYSTEMS

Software	Wind	Solar	Free trial	Technical	Economic	Optimization
RETScreen	✓	✓	✓	✓	✓	×
Hybrid2	✓	✓	✓	✓	×	×
SolSim	×	✓	×	✓	✓	✓
HYBRIDS	✓	✓	×	✓	×	✓
HYDROGEMS	✓	✓	×	✓	✓	✓
TRNsys	✓	✓	✓	✓	×	×
Ihoga	✓	✓	×	✓	✓	✓
pvSYSST	×	✓	✓	✓	×	✓
SAM	✓	✓	✓	✓	✓	×
HOMER	✓	✓	✓	✓	✓	✓

on-grid HESs based on PV/wind turbine/hydropower plant/hydrogen storage system for a rural area in Turkey were designed using the HOMER software. HES designs consisting of all and different combinations of PV/biogas generator/DG/BESS for a village in Xuzhou, China, were carried out in HOMER and compared in terms of cost and emissions [2].

To meet the energy demand of Maulana Azad National Institute of Technology Campus in Bhopal, Madhya Pradesh, India, the battery-included and off-grid rooftop PV system was designed using software such as SAM, Sunny Design, and Blue Sol [7]. Hillshade analysis was used to design an on-grid rooftop solar energy system for the building in Gangnam, Korea [8]. PVsyst and HOMER [9], PV*SOL, PVGIS, SolarGIS, and SISIFO [10] were used to analyze the performance of grid-connected rooftop PV systems.

In this paper, the design of a feasible grid-connected rooftop PV system, which takes into account real constraints such as roof area, component constraints, and annual load variation, is carried out in the HOMER program. This system, which is designed to provide emission mitigation and minimum energy costs, is modeled in Fig. 1. The design does not include any ESS, and when solar generation does not meet demand, energy is purchased from the grid, while excess solar energy is sold to the grid.

Main Points

- Increasing the use of renewable energy and reducing dependency on the grid and hence the dependence on fossil fuels.
- Providing more reliable analysis by using solar radiation data from three different sources such as the General Directorate of Meteorology, NASA, and PVGIS.
- Obtaining a feasible design by using real limit values such as roof area, photovoltaic panel dimensions, and component costs.
- Analyzing economic and environmental contributions using HOMER.
- As a future work, it is recommended to strengthen the design with components such as rooftop/wall-mounted wind turbines and battery energy storage systems.

The remainder of this paper is organized as follows. In Section II, the HOMER software and selected components are explained with their mathematical models. Section III covers the study location, energy consumption profile, and solar radiation data. The economic and environmental analysis of the grid-connected rooftop PV system is given in Section IV. Finally, the conclusion of this study and future work proposal are included in Section V.

II. METHODOLOGY AND COMPONENT MODELLING

A. HOMER Software

In this study, the HOMER software was used for rooftop PV system design and analysis. HOMER is an optimization tool developed by National Renewable Energy Laboratory for microgrid designs [11, 12]. Imitation, optimization, and sensitivity analysis are the basic functions in the HOMER software. HOMER considers the power

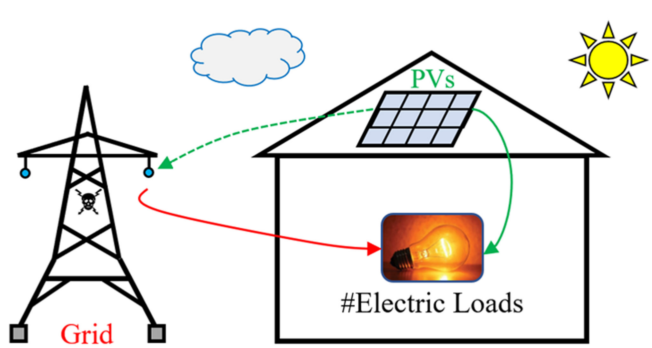

Fig. 1. Modeling of grid-connected rooftop PV system.

balance, load profile, location-specific tools, and system components all together and comprehensively and use the performance indicator such as cost of unit energy (CoE), net present cost (NPC), operational cost (OC), and initial cost [13].

CoE, which represents the cost of producing 1 kWh of electrical energy (unit energy), is the most critical indicator and is calculated as follows [14]:

$$CoE(\$/kWh) = \frac{TAC(\$/\text{year})}{TAEC(kWh/\text{year})} \quad (1)$$

where TAC represents the total annual cost and TAEC represents the total energy consumption per year.

NPC is the total of all expenses including capital, replacement, operation and maintenance, and fuel expenditures minus the salvage cost at the end of the project's lifetime. It is calculated as follows [13]:

$$NPC(\$/\text{year}) = \frac{TAC(\$/\text{year})}{CRF} \quad (2)$$

$$CRF(i,n) = \frac{i(1+i)^n}{(1+i)^n - 1} \quad (3)$$

where the capital recovery factor is represented by CRF, *i* is equal to the interest rate (%), and *n* is the lifetime of the components (year).

OC is calculated from the difference between the capital investment and the total annual cost and is expressed as follows [13, 14]:

$$OC(\$/\text{year}) = TAC(\$/\text{year}) - ACC(\$/\text{year}) \quad (4)$$

where ACC refers to the annual capital cost.

The solar savings fraction or solar fraction is the ratio of the energy supplied to the system by the PV panels to the total demand of the system and is calculated as a percentage as follows:

$$f_{solar} = \frac{E_{solar}}{E_{solar} + E_{grid}} \times 100 \quad (5)$$

where f_{solar} is the solar savings fraction, E_{solar} is the amount of solar energy generation, and E_{grid} is the amount of energy supplied from the grid.

B. PV Module

Since radiation and temperature are not constant in PV systems, also known as solar power systems, the output power also varies with time and can be calculated as follows:

$$P_{pv}(t) = N_{pv} \cdot P_{pv_r} \cdot f_{pv} \cdot \frac{G(t)}{G_n}\left[1 + \alpha_p\left(T_C(t) - T_{C_n}\right)\right] \quad (6)$$

where $P_{pv}(t)$ is the power output of the solar power system at time *t* (kW), N_{pv} is the number of the PV modules, P_{pv_r} is the nominal power of each PV module (kW), f_{pv} is the PV derating factor (%), $G(t)$ is the irradiation at the operating temperature at time *t* (kW/m^2), G_n is the irradiation at the standard test condition $(1kW/m^2)$, α_p is the temperature coefficient (%/°C), $T_C(t)$ is the cell temperature at time t (°C), and T_{C_n} is the nominal operating (test condition) temperature of the PV module (25°C).

TABLE II.
DATA OF SELECTED PV MODULES

Parameter	Specification
Manufacturer	Solar Energy SE 250/60P
Cell type	6″ polycrystalline
Cell dimension (H/W) (mm)	156×156
Number of cells	60 (10×6)
Panel dimension (H/W/D) (mm)	$1640 \times 992 \times 40$
Maximum power (W_p)	250
Weight (kg)	18
Open circuit voltage [U_{oc}] (V)	38.7
Short circuit current [I_{sc}] (A)	8.7
Voltage at maximum power [U_{mpp}] (V)	30.5
Current at maximum power [I_{mpp}] (A)	8.2
Panel efficiency (%)	15.4
Capital cost ($/kWp)	67.5
Replacement cost ($/kWp)	54
O&M cost ($/kWp/year)	10
Lifetime (years)	25

O&M, operating and maintenance; PV, photovoltaic.

TABLE III.
DATA OF THE INVERTER

Parameter	Specification
Manufacturer	CHINT POWER CPS SC100KT
Efficiency (%)	97.6
Capital cost ($/kWp)	8100
Replacement cost ($/kWp)	8100
O&M cost ($/kWp/year)	15
Lifetime (years)	15

O&M, operating and maintenance.

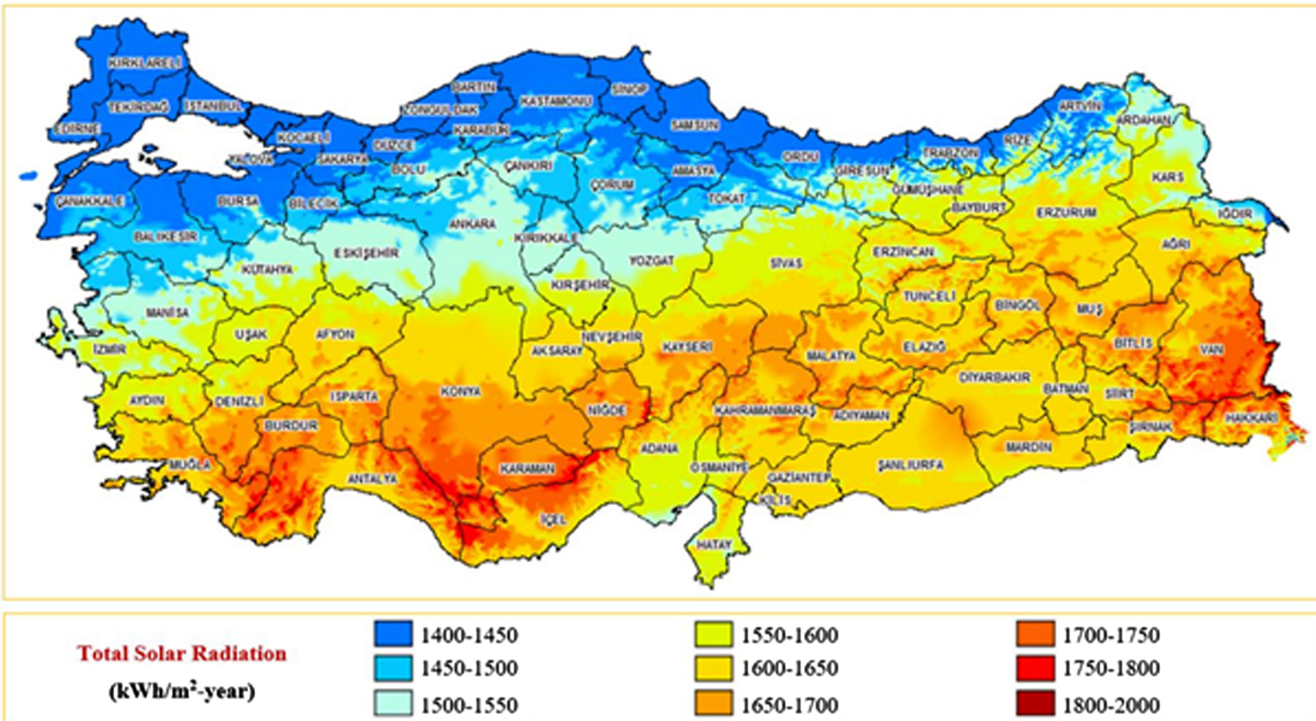

Fig. 2. Turkey's solar energy potential map.

In this study, the Solar Energy SE 250/60P model was selected from the HOMER database as the PV modules. Technical and economic data for the PV are given in Table II.

C. Converter

There are two types of energy conversion devices in HESs. The first converts from DC to AC and is called the inverter. The second converts from AC to DC and is called the rectifier [15].

In this study, the CHINT POWER CPS SC100KT model was selected from the HOMER database as the converter. Data for the converter are given in Table III.

III. STUDY LOCATION AND DATA

In this study, a grid-connected rooftop PV system was designed for the office building of a factory in Çerkezköy city, Tekirdağ province in Turkey. The location of Tekirdağ province and the solar potential map of Turkey are shown in Fig. 2 [16]. The office is located at 41°16′43′′ North latitude and 27°58′54′′ East longitude. Approximately 200 people work in the office building, which consists of office areas and test rooms, and electricity consumption is higher, especially between 08:00 and 18:00 during working hours. The monthly electricity consumption in the building in 2019 and 2020 is shown in Table IV and compared in Fig. 3.

Fig. 3 shows that the highest electricity consumption was in July for both years. This is due to the increase in air conditioning usage with the increase in temperatures in the summer months. On the other hand, there is a decrease in the electricity consumption data of 2020 compared to the consumption data of 2019, and this is explained as a result of the efforts made to save energy in the building.

TABLE IV.
MONTHLY TOTAL ELECTRICITY CONSUMPTION DATA OF THE OFFICE BUILDING

Months	2019 (kWh)	2020 (kWh)
January	103 638	117 092
February	96 694	108 310
March	113 292	111 533
April	106 081	96 744
May	128 826	97 139
June	132 056	115 020
July	136 603	141 758
August	136 551	134 996
September	135 407	137 504
October	123 919	129 012
November	123 043	106 771
December	118 212	105 861
Annual total	1 454 322	1 401 740

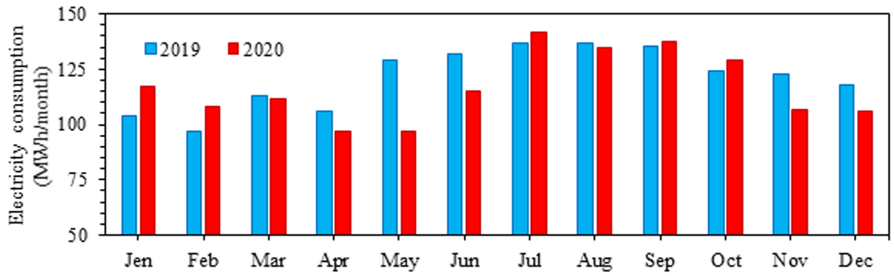

Fig. 3. Monthly electricity consumption data for 2019 and 2020.

In the HOMER software, it is required to enter the daily electricity consumption data hourly. By dividing the monthly consumption data by the number of days in each month, the average daily consumption data for each month can be obtained, and the average of these calculated values is equal to the average daily consumption of the whole year. The calculated average daily consumption values are given in Table V, and HOMER analyses were performed by taking the general average daily consumption of 3900 kWh.

Tekirdağ province temperature data is shown in Fig. 4, and the measurement period covers the years 1939–2020. By taking the average of the monthly temperature values measured during these years, the average temperature was determined as 14.1°C [17].

The measurement intervals for radiation data from the General Directorate of Meteorology (GDM), NASA, and PVGIS cover the years 2004–2018, 1983–2005, and 2005–2016, respectively. The average daily irradiance values were calculated as 3.92 kWh/m^2/day, 3.93 kWh/m^2/day, and 4.20 kWh/m^2/day, respectively. The average daily radiation and clearness indexes for the office building are shown in Fig. 5.

TABLE V.
DAILY AVERAGE ELECTRICITY CONSUMPTION DATA OF THE OFFICE BUILDING

Months	2019 (kWh)	2020 (kWh)
January	3343.16	3777.16
February	3453.36	3734.83
March	3654.58	3597.84
April	3536.03	3224.80
May	4155.68	3133.52
June	4401.87	3834.00
July	4406.55	4572.84
August	4404.87	4354.71
September	4513.57	4583.47
October	3997.39	4161.68
November	4101.43	3559.03
December	3813.29	3414.87
Annual average	3981.81	3829.06

IV. ANALYSIS AND RESULTS

From the image obtained from the Google Earth system, the PV panel applicable roof area was calculated as 2613.75 m^2. The roof area was divided into six parts named A, B, C, D, E, and F as shown in Fig. 6, and a separate module layout calculation was made for each area. While placing the PV modules, the modules were placed facing south in terms of location. The area, number of panels, and installed power are calculated for each zone and listed in Table VI.

Solar modules with 250 W power were used for the system design. The total number of modules calculated for the system is 485. Considering the power of the PV module used, it is predicted that the installed power of the system will be 485 × 250 = 121.250 kW.

HOMER designs the system by taking into account the economic data. The economic data entered are important for the accuracy of the simulation. As economic data, interest rate, inflation, real

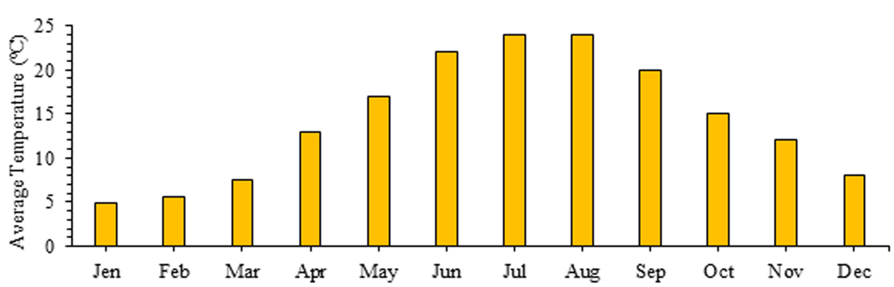

Fig. 4. Monthly average temperature values.

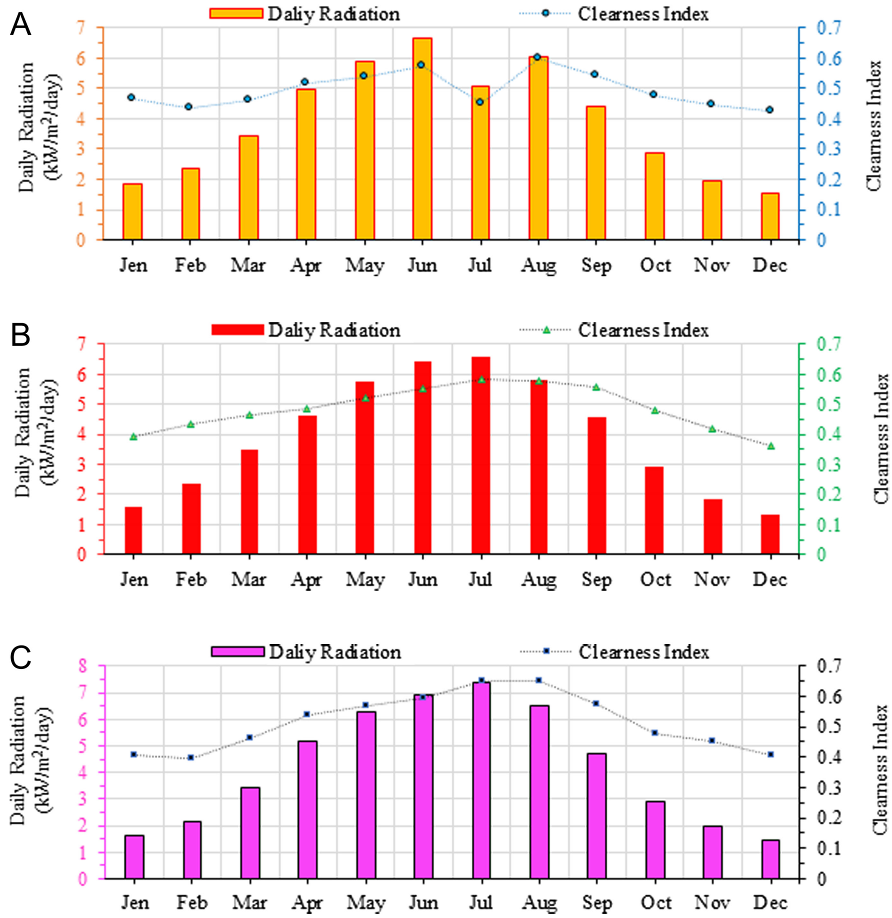

Fig. 5. Solar radiation data and clearness indexes from a) GDM, b) NASA, c) PVGIS.

interest rate, and project life data are required. Project life is taken as 25 years. This period is determined as the lifetime of the PV panel. Considering the data of the Central Bank of the Republic of Turkey for the last 10 years, the interest rate is 8% and the inflation rate is 10%. The real interest rate was found to be –1.82%. According to the electricity tariff effective as of April 1, 2021, announced by the Energy Market Regulatory Authority, the one-time electricity purchase price is 0.10634 $/kWh, and

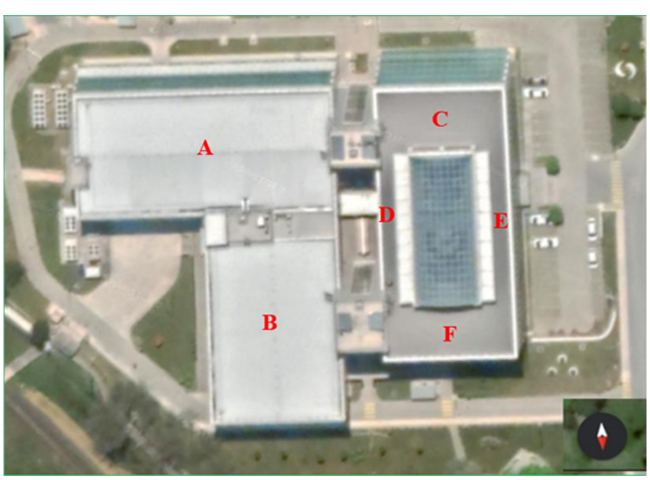

Fig. 6. Office building roof divided into 6 zones.

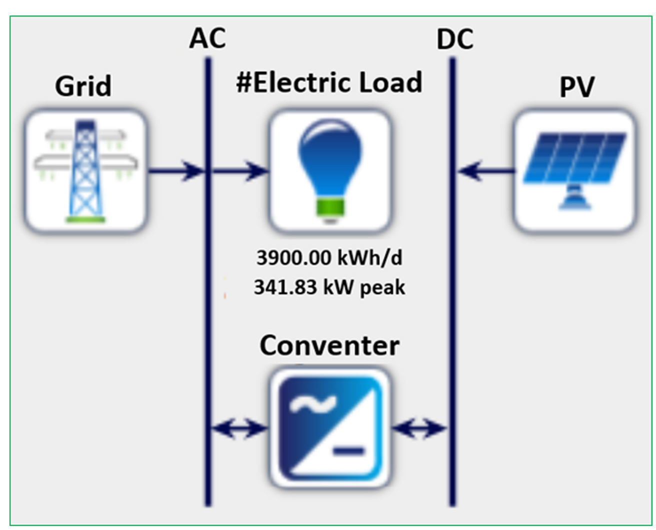

Fig. 7. On-grid PV system.

TABLE VI.
PLACEMENT OF PV MODULES IN REGIONS

Zone	Width (m)	Height (m)	Area (m²)	Number of arrays	Number of PVs in the array	Total number of PVs	Installed power (kWp)
A	46	24	1104	8	27	216	54
B	34	24	816	12	13	156	39
C	23.5	12.5	293.75	4	13	52	13
D	30	2.5	75	11	1	11	2.75
E	30	3	90	11	1	11	2.75
F	23.5	10	235	3	13	39	9.75
Total	–	–	2613.75	–	–	485	121.25

PV, photovoltaic.

TABLE VII.
THE RESULT OF THE COST ANAYLSIS

Data from	Component	Initial investment cost ($)	Replacement cost ($)	Operating & Maintenance cost ($)	Grid payment ($)	Scrap cost ($)	Total cost ($)
GDM	PV	121 250	0	38 816.20	0	0	160 066.20
	Grid	0	0	0	4 316 900.98	0	4 316 900.98
	Converter	21 375	28 142.52	41 057.13	0	11 272.19	79 302.46
	System	142 625	28 142.52	79 873.33	4 316 900.98	11 272.19	4 556 269.64
NASA	PV	121 250	0	38 816.20	0	0	160 066.20
	Grid	0	0	0	4 325 028.74	0	4 325 028.74
	Converter	21 375	28 142.52	41 057.13	0	11 272.19	79 302.46
	System	142 625	28 142.52	79 873.33	4 325 028.74	11 272.19	4 564 397.40
PVGIS	PV	121 250	0	38 816.20	0	0	160 066.20
	Grid	0	0	0	4 293 568.18	0	4 293 568.18
	Converter	21 375	28 142.52	41 057.13	0	11 272.19	79 302.46
	System	142 625	28 142.52	79 873.33	4 293 568.18	11 272.19	4 532 936.84

GDM, General Directorate of Meteorology; PV, photovoltaic.

TABLE VIII.
METRIC COMPARISON OF THE SIMULATION RESULT

Data from	PV (kW)	Converter (kW)	CoE ($/kWh)	NPC (M$)	OC ($)	IC ($)	Solar fraction (%)
GDM	121	85.5	0.1000	4.56	137 869	142 625	10.6
NASA	121	85.5	0.1000	4.56	138 123	142 625	10.5
PVGIS	121	85.5	0.0995	4.53	137 140	142 625	11.1

CoE, cost of energy; GDM, General Directorate of Meteorology; IC, initial cost; NPC, net present cost; OC, operating cost; PV, photovoltaic.

TABLE IX.
EMISSION COMPARISON BY DIFFERENT SOURCES OF RADIATION DATA

Emissions	Carbon dioxide (kg/year)	Sulfur dioxide (kg/year)	Nitrogen oxides (kg/year)
GDM	804.089	3.486	1.705
NASA	805.584	3.493	1.708
PVGIS	799.737	3.467	1.696

GDM, General Directorate of Meteorology.

the electricity sales price for unlicensed PV systems is 0.07354 $/kWh.

The system designed at HOMER to perform the economic and environmental analyses of the grid-connected rooftop solar energy system is shown in Fig. 7.

The results of the simulations made according to the GDM, NASA, and PVGIS data, cost analysis, and emission values are given in Tables VII, VIII, and IX, respectively.

Looking at these tables, since the roof area does not change, the number of PV, PV power, and converter power are the same for three different radiation data. Accordingly, the initial investment cost, replacement cost, operation and maintenance cost, and scrap costs of these components are the same. The solar fraction has increased in proportion to the average radiation value, and therefore the purchase of electrical energy from the grid has decreased. This situation led to a decrease in the total operating cost and thus a decrease in the CoE. In addition, for all three cases, the CoE is cheaper than the grid price, and there has been a significant reduction in emissions.

V. CONCLUSION

In this study, the economic and environmental benefits of installing a PV system with an installed power of 121.25 kW on the roof of a building in Çerkezköy, Tekirdağ, in Turkey were analyzed. Although the rooftop solar panel could not meet the entire energy demand of the office, a reduction of $8726 in annual bills and a reduction of 101.353 kg in emissions were calculated as a result of approximately 11% solar fraction obtained. It has been observed that even small applications of rooftop solar panels will have positive effects on our world in combating the devastating effects of both the energy crisis and the climate crisis. The renewable fraction and efficiency of the project can be increased by supporting the system with roof/wall type wind turbines or a suitable RES and ESSs.

Peer-review: Externally peer-reviewed.

Declaration of Interests: The authors haveno conflicts of interest to declare.

Funding: The authors declared that this study has received no financial support.

REFERENCES

1. M. Purlu, "Mikrobiyal Yakıt Hücreleri: Enerji Krizini Yenmek İçin Tercih Edilen Bir Teknoloji," içinde TEKNOBİLİM-2022: Enerji Krizi ve Yenilenebilir Enerji-II, C. Karaman, Ed. Türkiye; İstanbul: Efe Akademi Yayınları, 2022, ss. 83-100.
2. C. Li, L. Zhang, F. Qiu, and R. Fu, "Optimization and enviro-economic assessment of hybrid sustainable energy systems: The case study of a photovoltaic/biogas/diesel/battery system in Xuzhou, China," Energy Strategy Rev., vol. 41, p. 100852, 2022. [CrossRef]
3. Ö. Merev, "Feasibility of PV-based islanded microgrids for affordable electricity in sub-Saharan Africa," Turk J. Electr. Power Energy Syst., vol. 1, no. 2, pp. 60–68, 2021.
4. K. Buts, L. Dewan, and M. Prasad, "Design and control of a PV-FC-BESS-based hybrid renewable energy system working in LabVIEW environment for short/long-duration irrigation support in remote rural areas for paddy fields," Turk J. Electr. Power Energy Syst., vol. 1, no. 2, pp. 75–83, 2021.
5. T. O. Ajewole, O. Oladepo, K. A. Hassan, A. A. Olawuyi, and O. Onarinde, "Comparative study of the performances of three metaheuristic algorithms in sizing hybrid-source power system," Turk J. Electr. Power Energy Syst., vol. 2, no. 2, pp. 134–146, 2022.
6. M. Purlu, S. Beyarslan, and B. E. Turkay, "Optimal design of hybrid grid-connected microgrid with renewable energy and storage in a rural area in Turkey by using Homer," in 13th International Conference on Electrical and Electronics Engineering (ELECO), IEEE Publications, 2021, pp. 263–267. [CrossRef]
7. A. K. Shukla, K. Sudhakar, and P. Baredar, "Design, simulation and economic analysis of standalone roof top solar PV system in India," Sol. Energy, vol. 136, pp. 437–449, 2016. [CrossRef]
8. T. Hong, M. Lee, C. Koo, J. Kim, and K. Jeong, "Estimation of the available rooftop area for installing the rooftop solar photovoltaic (PV) system by analyzing the building shadow using hillshade analysis," Energy Procedia, vol. 88, pp. 408–413, 2016. [CrossRef]
9. N. Anang, S. N. A. Azman, W. M. W. Muda, A. N. Dagang, and M. Z. Daud, "Performance analysis of a grid-connected rooftop solar PV system in Kuala Terengganu, Malaysia," Energy Build., vol. 248, p. 111182, 2021. [CrossRef]
10. C. Dondariya et al., "Performance simulation of grid-connected rooftop solar PV system for small households: A case study of Ujjain, India," Energy Rep., vol. 4, pp. 546–553, 2018. [CrossRef]
11. J. Kumari, P. Subathra, J. E. Moses, and D. Shruthi, "Economic analysis of hybrid energy system for rural electrification using Homer," International Conference on Innovations in Electrical, Electronics, Instrumentation and Media Technology (ICEEIMT), IEEE Publications, 2017, pp. 151–156. [CrossRef]
12. S. Chauhan, R. Pande, and S. Sharma, "Techno-economic study of offgrid renewable energy system in Darma valley, Uttarakhand, India," Curr. Sci., vol. 9, p. 121, 2021.
13. M. Pürlü, S. Beyarslan, and B. E. Türkay, "On-grid and off-grid hybrid renewable energy system designs with Homer: A case study of rural electrification in Turkey," Turk J. Electr. Power Energy Syst., vol. 2, no. 1, pp. 75–84, 2022.
14. A. Abbassi, R. B. Mehrez, R. Abbassi, S. Saidi, S. Albdran, and M. Jemli, "Improved off-grid wind/photovoltaic/hybrid energy storage system based on new framework of Moth-Flame optimization algorithm," Int. J. Energy Res., vol. 46, no. 5, pp. 6711–6729, 2022. [CrossRef]
15. J. Huang, W. Li, L. Guo, X. Hu, and J. W. Hall, "Renewable energy and household economy in rural China," Renew. Energy, vol. 155, pp. 669–676, 2020. [CrossRef]
16. GEPA [online]. Available: https://gepa.enerji.gov.tr/MyCalculator/Default.aspx.
17. Meteoroloji Genel Müdürlüğü [online]. Available: https://www.mgm.gov.tr/veridegerlendirme/il-ve-ilceler-istatistik.aspx?m.